Polymer Films on Electrodes. 14. Spectral Sensitization of n-Type SnO_2 and Voltammetry at Electrodes Modified with Nafion Films Containing $Ru(bpy)_3^{2+}$

Mahadevaiyer Krishnan, Xun Zhang, and Allen J. Bard*

Contribution from the Department of Chemistry, The University of Texas at Austin, Austin, Texas 78712. *Received June 2, 1983. Revised Manuscript Received August 22, 1984*

Abstract: The spectral sensitization of n-type SnO_2 by $Ru(bpy)_3^{2+}$ incorporated in a perfluorosulfonate polymer (Nafion) matrix is described. The spectral response of the sensitized photocurrent is the same as the absorption spectrum of the Ru complex. The anodic photocurrent at the absorption maximum is higher for thin films (0.3–0.5 μm) than for thicker films (1–10 μm). The cyclic voltammetric behavior of the coated electrodes in the presence of solution redox couples indicates that the mediation of oxidation of the solution species is very efficient at thin film electrodes while practically no mediation is observed with thicker films. Rotating disk measurements allow a quantitative treatment of the processes that control the limiting currents in thin films. The quenching of the luminescence of incorporated $Ru(bpy)_3^{2+}$ by solution species with different permeability and at different states of oxidation of the Ru complex is also described.

Spectral sensitization of wide band gap semiconductor electrodes with organic dyes and organometallic complexes such as $Ru(bpy)_3^{2+}$ dissolved in solution has been the subject of several investigations in the past.[1-5] Such studies are of interest, not only because they provide an insight into the nature of charge transfer between electrodes and excited states, but also because sensitization permits the use of longer wavelength light for solar energy conversion. The main drawback in this approach is the low conversion efficiency resulting from the use of concentrated (e.g., millimolar) solutions to maintain adsorbed monolayers.[6,7] This reduces the sensitized photocurrents because the dye in the solution itself acts as an effective filter and decreases the intensity of the light at the electrode surface. Attempts have been made to overcome this problem by covalently attaching or adsorbing the sensitizer molecules to the electrode surface. Such surface modification can help to confine a high concentration of molecules to the surface while keeping the solution free of them to lessen the filter effect. Earlier studies[8,9] based on this approach indicate that in spite of the higher surface concentration, the efficiency is still low because only the first few monolayers near the electrode are electroactive. Although the subsequent layers were photoactive, they were unable to participate in the charge-transfer process.

Another important development[10-18] in surface modification is the use of polymer and polyelectrolyte coatings which can readily incorporate various ionic electroactive species into their matrices. Apart from the prolonged stability and strong attachments, an important feature of these films is that the quantity of electroactive material is generally in great excess of one monolayer. These polymer-coated electrodes bearing redox catalysts have been used to catalyze or mediate electron transfer between the electrode surface and reactants present in solution.[19] The charge propagation through the polymeric films is believed to occur by means of electron hopping between adjacent oxidized and reduced sites.[17,20] This electron hopping and the associated counterion motions can be regarded as a diffusion process.[20-22] For example, Saveant et al.[23] have proposed that the polymer film can be regarded as the statistical equivalent of several monolayers with charge transfer between the layers taking place through the hopping mechanism. According to this model the mediation at polymer electrodes can be more efficient than that at a monolayer derivatized electrode because several layers can participate actively in the charge-transfer process, and electroactive material in solution can penetrate the polymer layer. The efficiency will increase with increasing thickness of the film until mass transport of the solution species or electrons in the film becomes the limiting process. Since for practical application it is preferable to have a stable, thicker film containing higher concentrations of the active material, polymer-modified electrodes should be useful in photosensitization studies as well. Earlier reports from our laboratory[24,25] described polymer electrodes based on the ion-exchange polymer Nafion. The electron and mass transfer properties of this film have also been investigated in detail.[25] The advantages of combining both optical and electrochemical measurements to investigate the processes occurring at polymer film electrodes have been demonstrated recently.[26-29] This report describes the results of our

(1) Gerischer, H. *Photochem. Photobiol.* **1975**, *16*, 243, and references cited therein.
(2) Memming, R. *Photochem. Photobiol.* **1975**, *16*, 325, and references cited therein.
(3) Jaeger, C. D.; Fan, F. F.; Bard, A. J. *J. Am. Chem. Soc.* **1980**, *102*, 2592.
(4) Gleria, M.; Memming, R. *Z. Phys. Chem. (Frankfurt am Main)* **1976**, *98*, 303.
(5) Gleria, M.; Memming, R. *Z. Phys. Chem. (Frankfurt am Main)* **1976**, *101*, 171.
(6) Memming, R.; Schoppel, F.; Bringmann, U. *J. Electroanal. Chem.* **1979**, *100*, 307.
(7) Clark, W. D. K.; Sutin, N. *J. Am. Chem. Soc.* **1977**, *99*, 4676.
(8) Ghosh, P. K.; Spiro, T. G. *J. Am. Chem. Soc.* **1980**, *102*, 5543.
(9) Pool, K.; Buck, R. P. *J. Electroanal. Chem.* **1979**, *95*, 241.
(10) For a general review see: (a) Murray, R. W. *Acc. Chem. Res.* **1980**, *13*, 135. (b) Murray, R. W. "Electroanalytical Chemistry"; Bard, A. J., Ed.; Marcel Dekker: New York, 1984; Vol. 13. (c) Albery, W. J.; Hillman, A. R. *Chem. Soc. Annu. Rep. C* **1981**, 377-437.
(11) Miller, L. L.; Van de Mark, M. R. *J. Am. Chem. Soc.* **1978**, *100*, 639.
(12) (a) Merz, A.; Bard, A. J. *J. Am. Chem. Soc.* **1978**, *100*, 3222. (b) Itaya, K.; Bard, A. J. *Anal. Chem.* **1978**, *50*, 1487.
(13) (a) Lenhard, J. R.; Murray, R. W. *J. Am. Chem. Soc.* **1978**, *100*, 7870. (b) Nowak, R.; Schultz, F. A.; Umaña, M.; Abruña, H.; Murray, R. W. *J. Electroanal. Chem.* **1978**, *94*, 219.
(14) (a) Wrighton, M. S.; Austin, R. G.; Bocarsly, A. B.; Bolts, J. M.; Haas, O.; Legg, K. D.; Nadjo, L.; Palazzotto, M. C. *J. Am. Chem. Soc.* **1978**, *100*, 1602. (b) Wrighton, M. S.; Austin, R. G.; Bocarsly, A. B.; Bolts, J. M.; Haas, O.; Legg, K. D.; Nadjo, L.; Palazzoto, M. C. *J. Electroanal. Chem.* **1978**, *87*, 429. (c) Bolts, J. M.; Wrighton, M. S. *J. Am. Chem. Soc.* **1978**, *100*, 527. (d) Wrighton, M. S.; Palazzotto, M. C.; Bocarsly, A. B.; Bolts, J. M.; Fischer, A. B.; Nadjo, L. *Ibid.* **1978**, *100*, 7264.
(15) Oyama, N.; Anson, F. C. *J. Am. Chem. Soc.* **1979**, *101*, 739.
(16) Oyama, N.; Anson, F. C. *J. Electrochem. Soc.* **1980**, *127*, 247.
(17) Kaufman, F. B.; Engler, E. M. *J. Am. Chem. Soc.* **1979**, *101*, 541.
(18) Schroder, A. H.; Kaufman, F. B.; Patel, V.; Engler, E. M. *J. Electroanal. Chem.* **1980**, *113*, 193.
(19) Oyama, N.; Anson, F. C.; *Anal. Chem.* **1980**, *52*, 1192.
(20) Peerce, P. J.; Bard, A. J.; *J. Electroanal. Chem.* **1980**, *114*, 89.
(21) Laviron, E. *J. Electroanal. Chem.* **1980**, *112*, 1.
(22) Andrieux, C. P.; Saveant, J. M. *J. Electroanal. Chem.* **1980**, *111*, 377.
(23) Andrieux, C. P.; Dumas-Bouchiat, J. M.; Saveant, J. M.; *J. Electroanal. Chem.* **1980**, *114*, 159.
(24) (a) Rubinstein, I.; Bard, A. J. *J. Am. Chem. Soc.*, **1980**, *102*, 6641. (b) Rubinstein, I.; Bard, A. J. *Ibid.* **1981**, *103*, 5007.
(25) (a) Henning, T. P.; White, H. S.; Bard, A. J. *J. Am. Chem. Soc.* **1981**, *103*, 3937. (b) White, H. S.; Leddy, J.; Bard, A. J. *Ibid. Soc.* **1982**, *104*, 4811. (c) Martin, C. R.; Rubinstein, I.; Bard, A. J. *Ibid.* **1982**, *104*, 4817.
(26) Albery, W. J.; Boutelle, M. G.; Colby, P. J.; Hillman, A. R. *J. Electroanal. Chem.* **1982**, *133*, 135.
(27) (a) Buttry, D. A.; Anson, F. C. *J. Am. Chem. Soc.* **1982**, *104*, 4824. (b) Perry, J. W.; McQuillan, A. J.; Anson, F. C.; Zewal, A. H. *J. Phys. Chem.* **1983**, *87*, 1480.

0002-7863/84/1506-7371$01.50/0

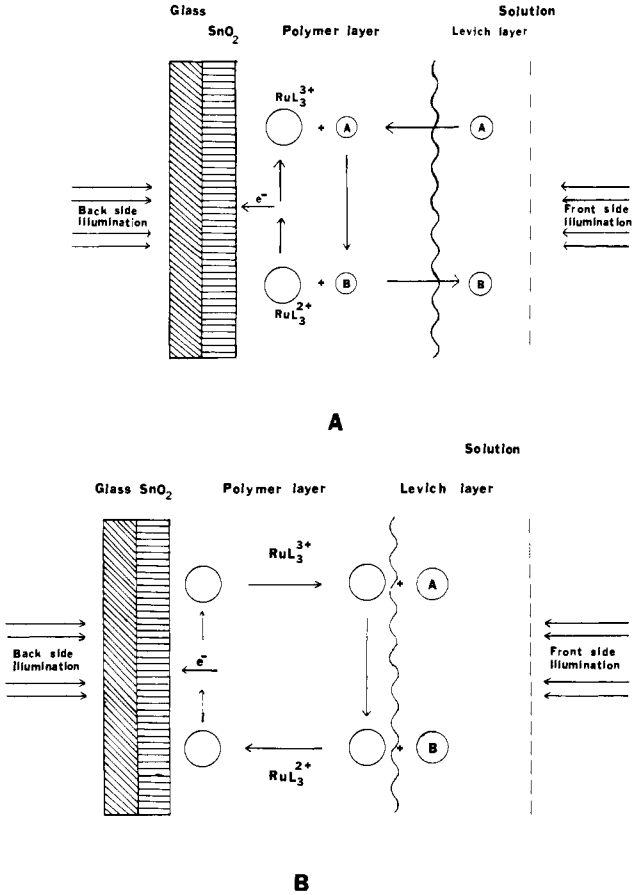

Figure 1. Schematic diagram of the photosensitization of n-type SnO_2 by polymer-bound $Ru(bpy)_3^{2+}$: (A) solution species can penetrate the polymer film, e.g., hydroquinone, Fe^{2+}; (B) solution species cannot penetrate the polymer film, e.g., $Fe(CN)_6^{4-}$ (thickness is not to scale).

efforts to use Nafion films containing $Ru(bpy)_3^{2+}$ for spectral sensitization of n-type SnO_2. Our aim is to identify and understand the nature of interfacial and polymer processes that influence the conversion efficiency of such systems.

A schematic representation of the polymer electrode in a photosensitization experiment is shown in Figure 1. The polymer layer coated over a conductive SnO_2 layer contains the sensitizing ruthenium complex. This polymer layer can be excited either directly through the solution (front-side illumination) or through the glass/SnO_2 layer (back-side illumination). In the case of back-side illumination, the layers adjacent to the electrode surface that can transfer charge to the electrode efficiently are irradiated well. In the front-side case, layers that are further from the SnO_2 are preferentially illuminated. To avoid any SnO_2 bandgap excitation, suitable UV cutoff filters were used. The excited molecules under favorable conditions transfer electrons to the SnO_2 semiconductor electrode producing the +3 form.

$$Ru(bpy)_3^{2+} \rightarrow Ru(bpy)_3^{2+*} \quad \text{(excitation)} \qquad (1)$$

$$Ru(bpy)_3^{2+*} \rightarrow Ru(bpy)_3^{3+} + e^- \quad \text{(electron transfer to electrode)} \qquad (2)$$

$$Ru(bpy)_3^{3+} + Red \rightarrow Ru(bpy)_3^{2+} + Ox \quad \text{(regeneration)} \qquad (3)$$

To improve the efficiency and regenerate the +2 form, a reducing agent, Red (supersensitizer), is added to the solution. The +2 form can be regenerated by the supersensitizer present in the solution when it penetrates the polymer to the SnO_2 interface. In this case the regeneration occurs inside the polymer matrix (Figure 1A). When the supersensitizer is unable to penetrate the polymer matrix, the oxidized (+3) molecules must reach the polymer film/electrolyte interface to be reduced by the solution species. Here, regeneration occurs at the film/solution interface (Figure 1B).

The net photocurrent intensity depends upon several factors. The production of excited states near the electrode surface occurs with back-side illumination. For front-side illumination, the concentration of excited states at the electrode surface depends upon film thickness. The molar absorptivity of $Ru(bpy)_3^{2+}$ is about 1.4×10^4 M^{-1} cm^{-1},[8] and its concentration in the films is about 0.2 to 0.5 M. Hence, with thick films (e.g., >1 μm), only a small amount of the radiation reaches the electrode/polymer interface with front-surface irradiation. In this case, the photocurrent will be influenced by the properties of the film, since the regeneration process depends upon the diffusion of the solution species across the film (case A) and on the diffusion-like propagation of charge in the polymer-bound species (cases A and B). Thus, by varying the film characteristics (such as thickness) and by a suitable choice of solution redox species, it is possible to investigate the nature of the processes that influence the energy conversion and transport processes at polymer film electrodes by both electrochemical and photochemical techniques.

Experimental Section

Materials. The 970 equivalent weight Nafion dissolved in ethanol 8% (w/v) was obtained from the E. I. DuPont de Nemours Co. All other chemicals (MCB) and $Ru(bpy)_3Cl_2 \cdot 6H_2O$ (Strem Chemicals, Newburyport, MA) were reagent grade and were used as received. Solutions were prepared from triply distilled water. SnO_2 conducting glass doped with Sb was cut into small (1 cm^2) pieces, cleaned with ethanol, soaked in 50% H_2SO_4 for 1 min, washed thoroughly with water, rinsed with alcohol, and dried.

Apparatus. The electrochemical cell with optically flat Pyrex windows with a saturated calomel reference electrode (SCE) and a platinum gauze counter electrode was used. Prepurified nitrogen was used for deaeration before the experiments. A Princeton Applied Research (PAR) Model 173 potentiostat and Model 175 universal programmer with a Model 179 digital coulometer were used for electrochemical experiments. The cyclic voltammograms were recorded with a Houston Instruments Model 2000 x-y recorder. The action spectra were recorded with a 2500-W xenon lamp, a power supply (Schoffel Instrument Co., Westwood, NJ), monochromator (Jarrel-Ash, Waltham, MA), PAR Model 192 variable frequency chopper, PAR Model 5204 lock-in amplifier, and Bascom-Turner 8110 recorder (Newton, MA). The photocurrent action spectra have been normalized against power output of the lamp-monochromator.

Rotating disk electrode (RDE) measurements were performed with a Pine Instruments ASR-2 rotator electrode assembly. The glassy carbon (area, 0.458 cm^2) electrode was hand-polished with Metadi-II (1 μm) diamond polishing compound (Buehler Ltd, Lake Bluff, IL), rinsed with ethanol, and air-dried before being coated with Nafion. Fluorescence measurements were made with a PAR Model 1216 optical multichannel analyzer system.

Procedures. Electrodes prepared from clean, dry SnO_2 glass had ohmic contacts to the conducting surface with silver-conducting paint (Acme Chemicals, New Haven, CT) and were sealed and mounted with 5-min Epoxy Cement (Devcon Corp., Danvers, MA) to a glass tube. Nafion was coated by covering the electrode surface with 30 μL of the ethanolic solution of appropriate dilution and allowing the solvent to evaporate.[24,25] The thickness of the dry films was determined with a Sloan-Dektak surface profilometer. Earlier measurements[25b] of film thickness before and after immersion in aqueous solutions of supporting electrolytes showed very little swelling of the film, and, hence, the film thickness in solution is taken to be equal to that of the measured dry thickness of the film. $Ru(bpy)_3Cl_2$ was incorporated by immersing the electrode in aqueous (5 mM) solutions for 30 min. The electrodes are then washed thoroughly with water several times. This procedure yielded films with a $Ru(bpy)_3^{2+}$ concentration of 0.2–0.5 M as determined from the integrated charge in a slow (5 mV/s) scan voltammetric experiment and the film thickness (0.3 μm). Such films will be denoted as SnO_2/NAF, $Ru(bpy)_3^{2+}$.

For RDE measurements films were cast by applying 20 μL of appropriate diluted ethanolic stock solution (8% w/v) onto the glassy carbon electrode and drying in air. Dry film thickness, as measured with the Sloan-Dektak surface profilometer, varied between 0.2 and 0.4 μm for thin films and between 2 and 4 μm for thick ones. Incorporation of $Ru(bpy)_3^{2+}$ into the film was accomplished by soaking the electrode in a 1 mM $Ru(bpy)_3Cl_2$ solution for more than 30 min. After soaking, the electrode was rinsed with distilled H_2O several times. The $Ru(bpy)_3^{2+}$

(28) Majda, M.; Faulkner, L. R. *J. Electroanal. Chem.* **1982**, *137*, 149.
(29) Oyama, N.; Yamaguchi, S.; Kaneko, M.; Yamada, A. *J. Electroanal. Chem.* **1982**, *139*, 215.

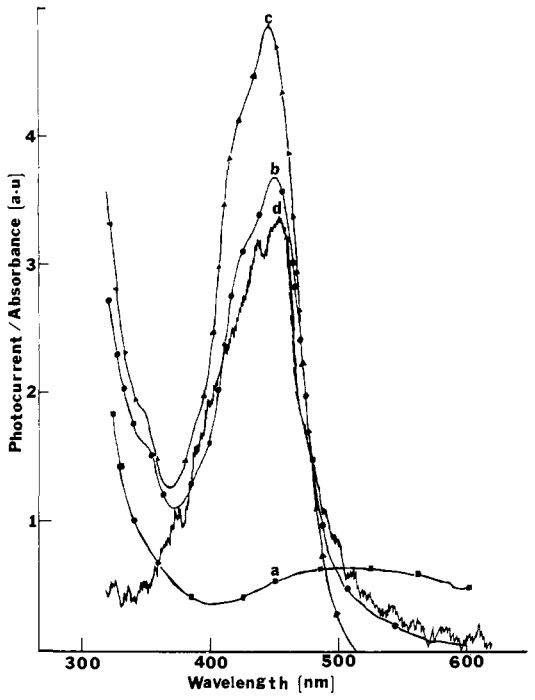

Figure 2. Comparison of the wavelength dependence of the polymer-bound $Ru(bpy)_3^{2+}$-sensitized anodic photocurrent with the absorption spectrum of $Ru(bpy)_3^{2+}$: (a) absorption spectrum of NAF-coated SnO_2; (b) absorption spectrum of polymer-bound $Ru(bpy)_3^{2+}$; (c) absorption spectrum of $Ru(bpy)_3^{2+}$ in solution; (d) anodic photocurrent action spectrum of SnO_2/NAF, $Ru(bpy)_3^{2+}$ in 0.1 N KCl containing 10 mM hydroquinone. Bias potential +0.2 V vs. SCE; photocurrent normalized with respect to the lamp spectrum.

surface concentration for thin films was 1.6×10^{-8} mol/cm^2 from coulometric measurements during a slow potential scan (1 mV/s). The electrode was immersed in pure supporting electrolyte for at least 0.5 h before each measurement to minimize the loss of $Ru(bpy)_3^{2+}$ to that solution during the experiment. All experiments were carried out under an inert (N_2) atmosphere.

Nafion films were checked for cracks or pinholes by observing the film behavior in presence of 1 mM $K_3Fe(CN)_6$. Since $Fe(CN)_6^{3-}$ ions do not penetrate Nafion films (as discussed in the Results section), no peak corresponding to the reduction of $Fe(CN)_6^{3-}$ should be observed in good, crack-free, films. Whenever peaks caused by $Fe(CN)_6^{3-}$ were observed at Nafion-coated electrodes, these electrodes were rejected.

Thick films ($\sim$3 μm) were made by two methods. In the first method, an amount of Nafion solution sufficient for the desired film thickness was placed on the electrode and allowed to dry; then $Ru(bpy)_3^{2+}$ was incorporated. In the second method, a thick layer was built by forming several thin layers of Nafion and loading with $Ru(bpy)_3^{2+}$. The latter films showed an increased tendency to develop cracks and tended to peel off. The general electrochemical behavior of thick films prepared by both methods was essentially the same.

Results and Discussion

Photosensitization Experiments. In Figure 2, we compare the anodic photocurrent action spectrum of the SnO_2/NAF, $Ru(bpy)_3^{2+}$ electrode with the absorption spectra of $Ru(bpy)_3^{2+}$ in solution and in the polymer film coated over SnO_2 glass. The wavelength dependence of the action spectrum corresponds closely to the absorption spectrum of the complex in the polymer and that in solution, showing that the photocurrent arises from the excitation of the ruthenium(II) complex. The photocurrent action spectra for thin ($\simeq$0.3 μm (A)) and thick ($\simeq$3 μm (B)) films coated over SnO_2 electrodes with illumination from the front (1) and back (2) sides are given in Figure 3. For the thick films, the photocurrents are much smaller (less than 1/4) than those of the thinner films. Moreover, while the photocurrents are essentially the same for front and back illumination in the thin films, for thick films much larger currents are found for back-side illumination (Figure 3B). In the thick films only a small fraction of the light reaches the electrode surface for front-side illumination while the thinner films are almost uniformly illuminated throughout their thickness.

The photocurrent intensity at the absorption maximum (λ 450 nm) as a function of the dry thickness of the polymer layer for back-side illumination (Figure 4) shows an essentially constant photocurrent for thicknesses below 0.3 μm which decreases steadily as the thickness increases. Since the polymer layer was excited through the glass/SnO_2 layer (back illumination), the observed behavior cannot be attributed to a decrease in light intensity at the electrode surface (an optical filter effect), but rather must be caused by slow charge transport in the film or at the solution interface. The dependence of photocurrent on film thickness showed the same trend for different redox species, $Fe(CN)_6^{4-}$/$Fe(CN)_6^{3-}$ and Fe^{2+}/Fe^{3+}, in solution. The same effect, with much lower photocurrents was observed when front-side illumination was employed.

Several processes might become rate determining as the film thickness is increased. Electron transfer between the dye in the first layer and the electrode is probably rapid. The transport of electrons from the subsequent layers may take place by the hopping mechanism, i.e., an exchange of electrons between adjacent reduced and oxidized centers together with a concurrent motion of counterions. Electron propagation across the whole film becomes increasingly difficult as the thickness increases; either the electron exchange between electroactive centers or the diffusion of counterions in the polymer matrix then becomes the rate-limiting step as mentioned earlier. Following transfer of an electron by $Ru(bpy)_3^{2+*}$ to the electrode (eq 2), the $Ru(bpy)_3^{3+}$ produced must ultimately be reduced by solution species to maintain the photocurrent. Hence, the 3+ form must move to the polymer/solution

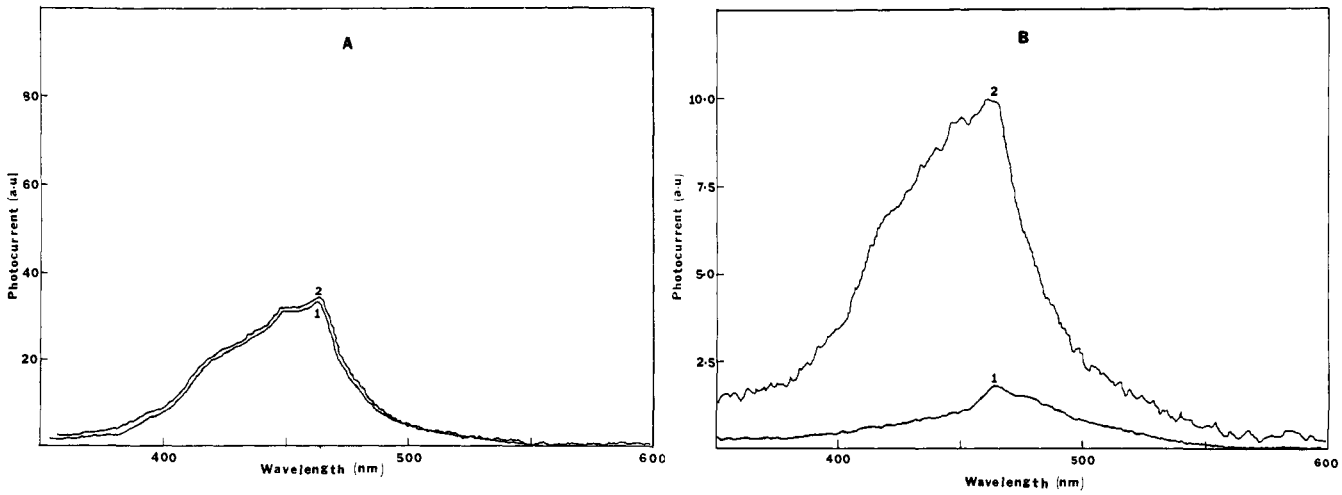

Figure 3. Effect of film thickness on the intensity of photocurrent (A) thin film (d = 0.3 μm); (B) thick film (d = $\sim$3 μm): (1) front illumination, (2) back illumination. Films contain 0.5 M $Ru(bpy)_3^{2+}$ and solution is 0.1 M KCl + 1 mM hydroquinone.

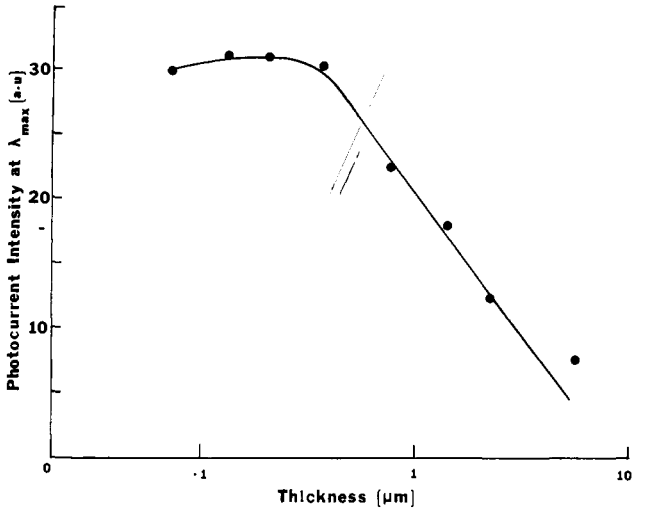

Figure 4. Normalized anodic photocurrent intensity at 450 nm as a function of film thickness with back-side illumination: bias potential +0.2 V vs. SCE; electrolyte 0.1 N KCl + 10 mM hydroquinone.

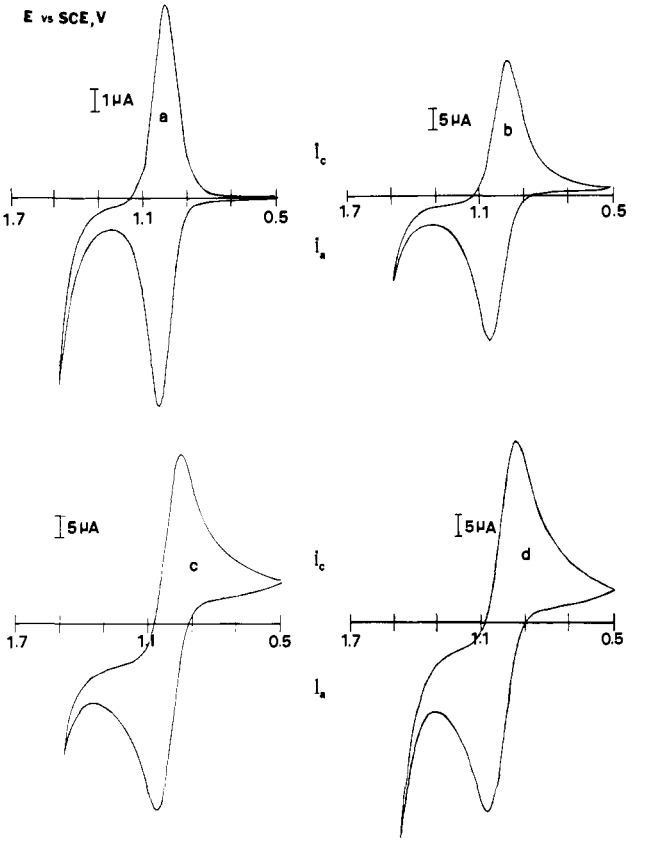

Figure 5. Cyclic voltammetry of SnO_2/NAF, $Ru(bpy)_3^{2+}$ in 0.1 M KCl at various thicknesses of the polymer film: scan rate, 5 mV/s; thickness, (a) 0.3 μm, (b) 0.73 μm, (c) 1.45 μm, (d) 3 μm. Cathodic currents are plotted as positive.

interface (via actual diffusion and/or electron hopping[25]) and the reduced solution species (e.g., H_2Q) must move toward the electrode surface. Moreover, the electron transfer of eq 2 requires the movement of counterions to maintain electroneutrality.

Regeneration of the $Ru(bpy)_3^{2+}$ depends on the concentration of the reducing agent in the polymer, which is controlled by its diffusion across the film from the solution side. In most cases, a partition equilibrium may also be involved. To examine in detail the various processes that are likely to limit the photoconversion efficiency, electrochemical (cyclic and RDE voltammetry) and luminescence experiments were carried out.

Cyclic Voltammetry. The shape of the cyclic voltammetric waves for the SnO_2/NAF, $Ru(bpy)_3^{2+/3+}$ depends on film

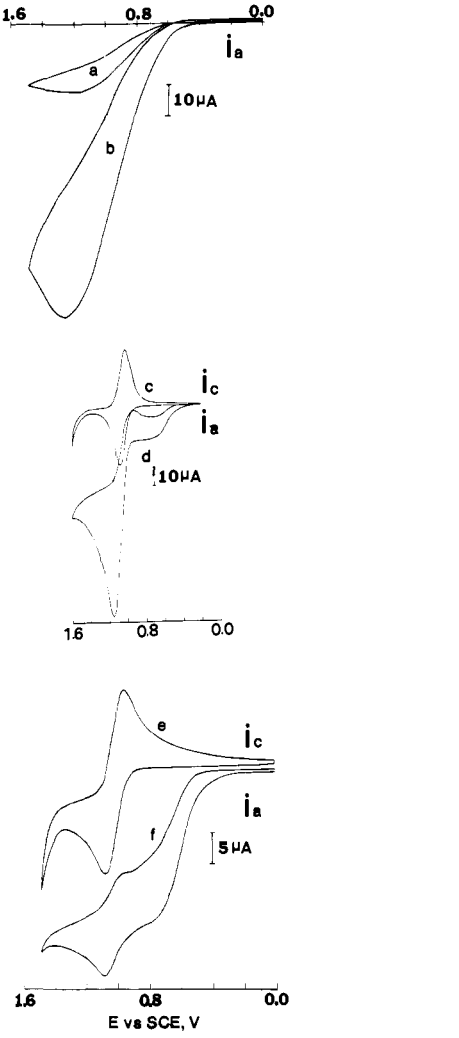

Figure 6. Cyclic voltammetry in 0.1 M KCl: (a) SnO_2/NAF (~0.5 μm) electrode in 1 mM hydroquinone; (b) SnO_2 in 1 mM hydroquinone; (c) SnO_2/NAF, $Ru(bpy)_3^{2+}$ in base electrolyte (d = 0.3 μm); (d) same electrode as (c) with 1 mM hydroquinone added to the solution; (e) SnO_2/NAF, $Ru(bpy)_3^{2+}$ thick film (d = 3 μm) electrode in base electrolyte; (f) same electrode as (e) with 1 mM hydroquinone added to solution. Scan rate 10 mV/s.

thickness (Figure 5); similar effects were previously seen for these films on a carbon substrate.[25] Note that the typical thin-layer behavior changes to a diffusion-controlled behavior as the film thickness increases at a given scan rate (5 mV/s). Clearly, complete conversion of all the incorporated $Ru(bpy)_3^{2+}$ into $Ru(bpy)_3^{3+}$ becomes difficult because of the interference of the kinetics of electron transfer through the film as the thickness is increased. Similar effects were observed when the sweep rate was varied at a given thickness. The effect of the addition of 1 mM hydroquinone (H_2Q) to the solution on the cyclic voltammograms of SnO_2/NAF, $Ru(bpy)_3^{2+}$ is shown in Figure 6. Also included in this figure are the waves corresponding to the direct oxidation of H_2Q on a bare SnO_2 (curve b) electrode and a Nafion-coated SnO_2 electrode (curve a). Oxidation of H_2Q on the bare electrode proceeds smoothly. H_2Q can be oxidized through the Nafion film; however, the peak currents are smaller by a factor of 3 or 4, depending on the thickness of the film, than on the same bare electrode. The current due to direct oxidation of H_2Q becomes smaller when $Ru(bpy)_3^{2+}$ is incorporated into the film (compare curves a and d); the current is about 10% of the bare electrode value for the same H_2Q concentration and geometric area of electrode, when the film is loaded with $Ru(bpy)_3^{2+}$. We attribute this smaller current to cross-linking introduced when several SO_3^- tails in Nafion are tied together by the incorporated $Ru(bpy)_3^{2+}$, thus slowing down the movement of H_2Q across the film. Note, however, that the wave for the direct oxidation of H_2Q is somewhat

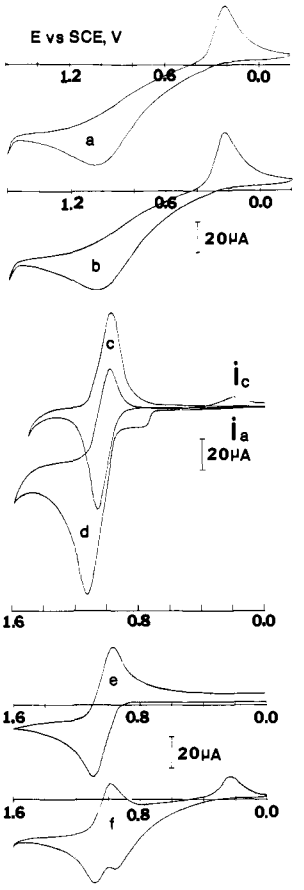

Figure 7. Cyclic voltammetry in 0.1 M Na_2SO_4 + 0.01 M H_2SO_4 at sweep rate 10 mV/s: (a) SnO_2 electrode in 1 mM $FeSO_4$; (b) SnO_2/NAF (d = 0.42 μm) in 1 mM $FeSO_4$; (c) SnO_2/NAF, $Ru(bpy)_3^{2+}$ in base electrolyte (d = 0.3 μm); (d) same electrode as (c) with 1 mM $FeSO_4$ added to the solution; (e) SnO_2/NAF, $Ru(bpy)_3^{2+}$ thick film (d = 3 μm) in base electrolyte; (f) same electrode as (e) with 1 mM $FeSO_4$ added to the solution.

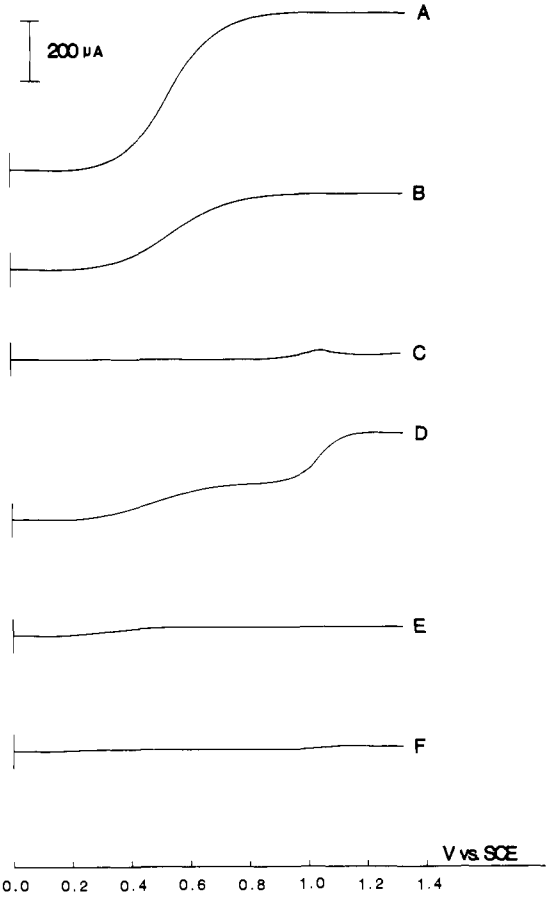

Figure 8. Cyclic voltammetry in 0.1 KCl at 10 mV/s: (a) SnO_2 electrode in 1 mM $K_4Fe(CN)_6$; (b) SnO_2/NAF (d = 0.4 μm) in 1 mM $K_4Fe(CN)_6$; (c) SnO_2/NAF, $Ru(bpy)_3^{2+}$ in base electrolyte (d = 0.3 μm); (d) same electrode as (c) with 1 mM $K_4Fe(CN)_6$ added to the solution; (e) SnO_2/NAF, $Ru(bpy)_3^{2+}$ thick film electrode in base electrolyte; (f) same electrode with 1 mM $K_4Fe(CN)_6$ added to the solution.

sharper and occurs at less positive potentials in the presence of $Ru(bpy)_3^{2+}$. A similar effect of $Ru(bpy)_3^{2+}$ is observed for the solution-phase oxidation of H_2Q at SnO_2 electrodes and is apparently caused by a small amount of adsorption of the Ru species which promotes electrochemical oxidation of H_2Q (i.e., heterogeneous electrocatalysis). The incorporated $Ru(bpy)_3^{2+}$ increases the rate of H_2Q oxidation at more positive potentials through mediation by the $Ru(bpy)_3^{3+/2+}$ couple (compare curves c and d). Thus, although direct oxidation of H_2Q begins at about +0.4 V (curve d), the current is limited by the rate of penetration of H_2Q through the film. However, when oxidation of $Ru(bpy)_3^{2+}$ occurs (at about +1.15 V), the anodic peak current is greatly increased because of the reaction between $Ru(bpy)_3^{3+}$ and H_2Q, regenerating the +2 form (a "catalytic" reaction sequence). The increased net current for H_2Q oxidation can be ascribed to the more rapid electron-transfer-type "diffusion" through the film.[25,27] Note that, in the presence of H_2Q, the cathodic peak corresponding to $Ru(bpy)_3^{3+}$ reduction is nearly absent. The film thickness in the above experiments was 0.3 μm, and the surface concentration of $Ru(bpy)_3^{2+}$ $\Gamma_0 = 4.3 \times 10^{-9}$ mol/cm^2.

The behavior at thicker films ($d \simeq 3$ μm and $\Gamma_0 = 3.7 \times 10^{-8}$ mol/cm^2) (Figure 6, curves e and f) often did not follow directly from that seen at thinner films. The current for the direct oxidation of H_2Q in the $Ru(bpy)_3^{2+}$-containing film sometimes appeared larger in the thicker films, and there was little or no enhancement of the anodic peak at +1.15 V (i.e., electrogenerated $Ru(bpy)_3^{3+}$ is not appreciably reduced back to the 2+ state by the H_2Q).

The larger currents for direct oxidation of H_2Q occurred only in thicker films loaded with $Ru(bpy)_3^{2+}$ but not in unloaded films of the same thickness. This appears to be caused by inefficient loading and cross-linking by $Ru(bpy)_3^{2+}$ in the thicker films.

Cyclic voltammograms corresponding to Fe^{2+}/Fe^{3+} oxidation at a Nafion-modified electrode are shown in Figure 7. Curves a and b correspond to the oxidation Fe^{2+} on a bare (a) and Nafion-coated electrodes (b); obviously, the Fe^{2+} has little difficulty penetrating the Nafion film. Again, addition of $Ru(bpy)_3^{2+}$ affects the film properties. Curves c and d indicate that oxidation of Fe^{2+} does not occur at the usual potential but is shifted to the Ru(II/III) potential at a modified electrode. Reduction of Fe^{3+} also appears to be hindered. This is again a result of a greater cross-linking and competition for cationic sites by $Ru(bpy)_3^{2+}$ which prevents Fe^{2+} penetration in the film. At the thicker film electrodes, Fe^{2+} oxidation appears to be uncatalyzed (curves e and f); the $Ru^{2+/3+}$ wave appears to be superimposed on the $Fe^{2+/3+}$ wave. Curve f also indicates incomplete incorporation and poorer cross-linking in the thick film, with a larger current for the direct oxidation of Fe^{2+}.

In Figure 8, curves a and b correspond to the direct oxidation of $Fe(CN)_6^{4-}$ on a bare SnO_2 electrode and on a Nafion-coated electrode. Absence of any oxidation current at the coated electrode indicates that $Fe(CN)_6^{4-}$ does not penetrate the polymer film. Upon incorporation of $Ru(bpy)_3^{2+}$, the $Fe(CN)_6^{4-}$ oxidation is catalyzed as shown by the change in the appearance of the $Ru(bpy)_3^{3+/2+}$ wave. The peak current in curve d approximately corresponds to the sum of the anodic peak currents of curves a and c. Thus, although $Fe(CN)_6^{4-}$ cannot penetrate the film, transport of $Ru(bpy)_3^{3+}$ to the film/solution interface allows oxidation of ferrocyanide and regeneration of $Ru(bpy)_3^{2+}$. However, again in a thicker film (curves e and f) no catalysis occurs at these sweep rates. Thus, it appears that irrespective of the ability of the solution species to penetrate through the polymer film, efficient reconversion of $Ru(bpy)_3^{3+}$ into $Ru(bpy)_3^{2+}$ is

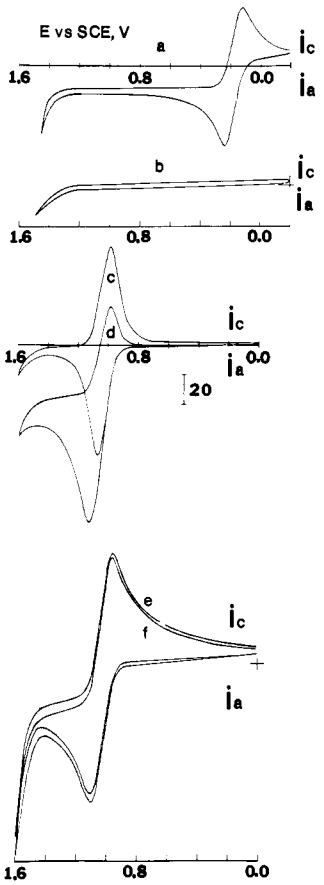

Figure 9. Voltammetry at GC RDE in 0.1 M Na_2SO_4 at scan rate 5 mV/s and rotation rate 1000 rpm: (A) bare GC RDE with 1 mM hydroquinone; (B) GC/NAF (d = ~0.3 μm) with 1 mM hydroquinone; (C) GC/NAF, $Ru(bpy)_3^{2+}$ (d = ~0.3 μm) in base electrolyte alone; (D) GC/NAF, $Ru(bpy)_3^{2+}$ (d = ~0.3 μm) with 1 mM hydroquinone; (E) GC/NAF (d = ~3 μm) with 1 mM hydroquinone; (F) GC/NAF, $Ru(bpy)_3^{2+}$ (d = ~3 μm) with 1 mM hydroquinone.

possible only for thin films. At higher film thicknesses (>3 μm) the efficiency decreases and almost no regeneration occurs. The electrochemical behavior at these films depends on film thickness and the ability of solution species to penetrate the films. A more quantitative treatment of the processes occurring at these electrodes under steady-state solution mass transport conditions can be obtained by rotating disk electrode (RDE) measurements.

Rotating Disk Electrode Measurements. Current potential (i–E) curves for a 1 mM solution of hydroquinone (H_2Q) in 0.1 M Na_2SO_4, at a glassy carbon RDE, are shown in Figure 9. Curve A corresponds to the oxidation of H_2Q at a bare electrode and curve B shows the effect of the presence of a thin Nafion film. The limiting current decreases in the presence of a film in comparison to its value at a bare electrode. This decrease is indicative of the extent of penetration of H_2Q into the Nafion film. Curve C represents the response of the GC/NAF, $Ru(bpy)_3^{2+}$ electrode in the pure supporting electrolyte. The redox potential for the bound $Ru(bpy)_3^{2+/3+}$ couple is observed at about +1.1 V vs. SCE. Curve D shows the same electrode as in C, but in 1 mM hydroquinone solution. Here the mediation of hydroquinone oxidation by the polymer-bound $Ru(bpy)_3^{2+}$ is clearly indicated by the shape of the (i–E) curve. The decrease in the limiting current for the direct oxidation of H_2Q again demonstrates that the penetration of H_2Q through the Nafion film is reduced by the introduction of $Ru(bpy)_3^{2+}$ into the polymer. Curves E and F are the responses of thick films in the absence and the presence of bound $Ru(bpy)_3^{2+}$ in a 1 mM H_2Q solution, respectively. A comparison of curves B and E shows that the direct oxidation of H_2Q through a thick film on a GC electrode that is saturated with $Ru(bpy)_3^{2+}$ is almost totally impeded. Note the absence of the mediation of H_2Q oxidation by the bound $Ru(bpy)_3^{2+}$ (curve F).

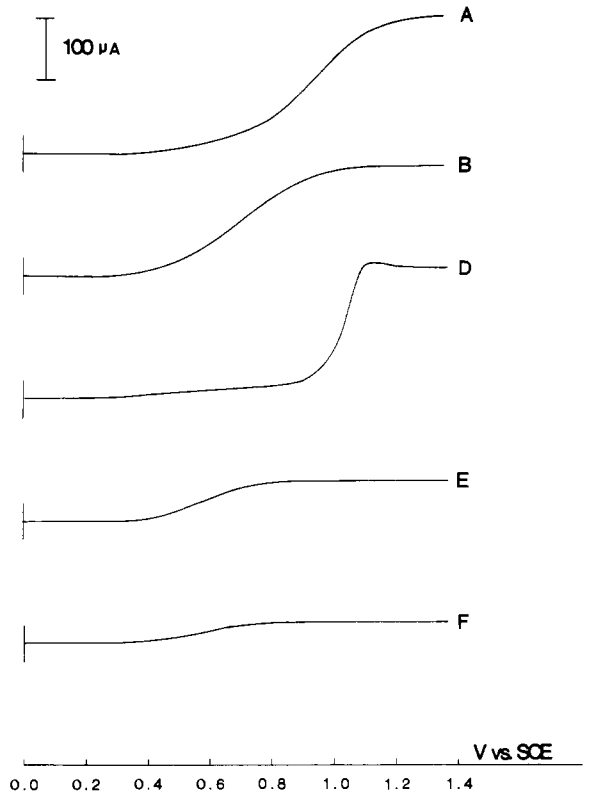

Figure 10. Voltammetry at GC RDE in 1 mM $FeSO_4$ + 0.1 M Na_2SO_4 + 0.01 M H_2SO_4 at scan rate 5 mV/s and rotation rate 1000 rpm: (A) bare GC RDE; (B) GC/NAF (d = ~0.3 μm); (C) see Figure 9; (D) GC/NAF, $Ru(bpy)_3^{2+}$ (d = ~0.3 μm); (E) GC/NAF (d = ~3 μm); (F) GC/NAF, $Ru(bpy)_3^{2+}$ (d = ~3 μm).

Current–potential curves for a 1 mM $FeSO_4$ solution in 0.1 M Na_2SO_4 containing 0.01 M H_2SO_4 are shown in Figure 10. The general behavior is similar to that observed in H_2Q solutions. However, a comparison of the limiting currents in curves A and B indicates that Fe^{2+} oxidation at the electrode is hardly affected by the presence of the Nafion film. The mechanism of Fe^{2+} penetration through the Nafion film is different from that of H_2Q, and Fe^{2+} oxidation at the polymer-coated electrode occurs at less positive potentials. Curve D shows the response of Fe^{2+} oxidation via $Ru(bpy)_3^{2+}/Ru(bpy)_3^{3+}$ mediation. A comparison of curve D in Figure 9 to curve D in Figure 10 shows that the limiting current for the direct oxidation of Fe^{2+} is lowered more than that for H_2Q by the incorporation of $Ru(bpy)_3^{2+}$ into the film. The difference can be explained as follows. Fe^{2+} ions enter the Nafion film by an ion-exchange mechanism, while H_2Q probably penetrates via the polymer backbone. The $Ru(bpy)_3^{2+}$ ions introduced in Nafion are tightly bound to SO_3^- sites in the polymer matrix, and this may also cause cross-linking. Moreover, the affinity of SO_3^- terminals for $Ru(bpy)_3^{2+}$ is higher than for Fe^{2+}, so that Fe^{2+} cannot replace bound $Ru(bpy)_3^{2+}$ ions. Diffusion of Fe^{2+} through the film is, therefore, strongly hindered by the presence of $Ru(bpy)_3^{2+}$. On the other hand, cross-linking by $Ru(bpy)_3^{2+}$ only partially blocks access of the hydroquinone to the GC surface. Curves E and F are the cases of thick films. Again, thick films do not show mediation of the substrate oxidation.

Curves in Figure 11 show the responses of the electrode in $K_4[Fe(CN)_6]$ solution. Absence of the direct oxidation wave in curve B results from the rejection of $Fe(CN)_6^{4-}$ ions by the Nafion film. Clearly, the $Ru(bpy)_3^{2+}/Ru(bpy)_3^{3+}$ mediated electron-transfer shown in curve D is the only way that $Fe(CN)_6^{4-}$ can be oxidized at the polymer-coated electrode. Mediation is absent at an electrode coated with thick films (curves E and F).

Analysis of Rotating Disk Electrode Results. The behavior of the RDE limiting current, i_l, as a function of rotation rate, ω [where ω (s^{-1}) = 2π (revolutions s^{-1})], and concentration of substrate in solution, C_A°, and of mediator in film, C_p°, can provide

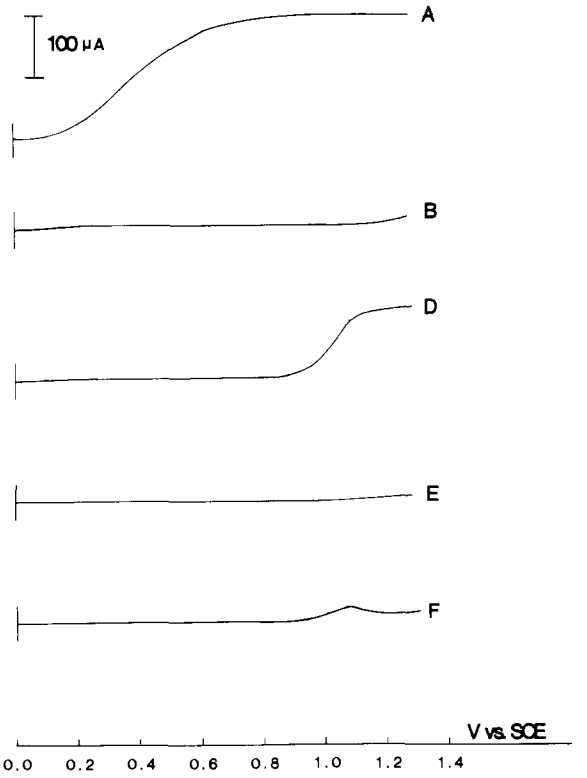

Figure 11. Voltammetry at GC RDE in 1 mM $K_4[Fe(CN)_6]$ + 0.1 M Na_2SO_4 at scan rate 5 mV/s and rotation rate 1000 rpm: (A) bare GC RDE; (B) GC/NAF (d = ~0.3 μm); (C) see Figure 9; (D) GC/NAF, $Ru(bpy)_3^{2+}$ (d = ~0.3 μm); (E) GC/NAF (d = ~3 μm); (F) GC/NAF, $Ru(bpy)_3^{2+}$ (d = ~3 μm).

Table I. Diffusion Coefficients of the Solution Species Calculated from the Plots of i_l^{-1} vs. $\omega^{-1/2}$: a Comparison between the Results at Bare GC RDE and at GC/NAF, $Ru(bpy)_3^{2+}$ RDE[a]

	diffusion coefficient, D_A, ($\times 10^5$ cm^2/s) at soln concn (C_A°) ($\times 10^6$ mol/cm^3)			
	0.10	0.20	0.50	1.00
	Bare GC RDE			
H_2Q	0.80	0.78	0.81	0.81
Fe^{2+}	0.79	0.76	0.73	0.70
$Fe(CN)_6^{4-}$	0.54	0.52	0.52	0.50
	GC/NAF, $Ru(bpy)_3^{2+}$ RDE			
H_2Q	0.83	0.77	0.80	
Fe^{2+}	0.81	0.73	0.70	0.70
$Fe(CN)_6^{4-}$	0.54	0.53	0.51	0.50

[a] Supporting electrolyte: H_2Q and $Fe(CN)_6^{4-}$: 0.1 M Na_2SO_4; Fe^{2+}: 0.1 M Na_2SO_4 + 0.01 M H_2SO_4

information about the mechanism of charge transfer in the films.[30] At bare electrodes, plots of i_l^{-1} vs. $\omega^{-1/2}$ [Koutecky–Levich (K–L) plots] are linear with slopes proportional to C_A° when the mass transfer rate of the solution species to the electrode surface controls the current.[31a] In general, when the current is limited by mass transport in solution and by a kinetic process at the electrode surface, the limiting current can be written as[31b]

$$(1/i_l) = (1/i_A) + (1/i_{kin}) \quad (4)$$

where i_A represents the rate of mass transfer at the RDE:

$$i_A = nFA(0.62)D^{2/3}\nu^{-1/6}C_A^\circ\omega^{1/2} \quad (5)$$

and i_{kin}, the kinetic current; e.g., at a bare electrode, the effect

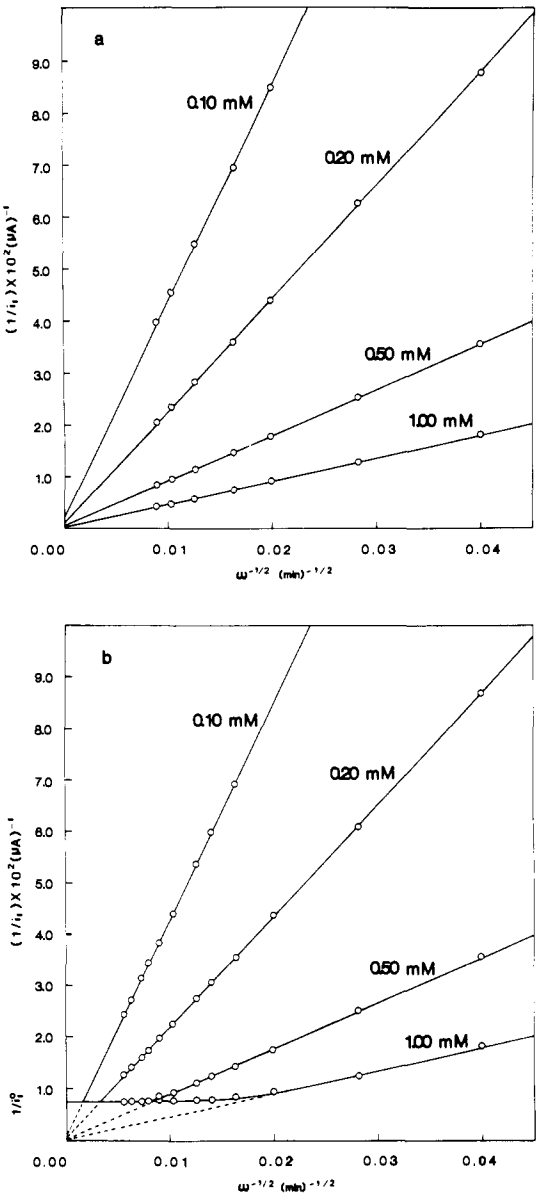

Figure 12. Plots of (limiting current)$^{-1}$, i_l^{-1}, vs. $\omega^{-1/2}$ (angular frequency of rotation)$^{-1/2}$, for the oxidation of $K_4[Fe(CN)_6]$ in 0.1 M Na_2SO_4: (a) bare GC RDE at E = +0.8 V vs. SCE; (b) GC/NAF, $Ru(bpy)_3^{2+}$ (d = ~0.3 μm) at E = +1.25 V vs. SCE.

of heterogeneous electron-transfer kinetics yields $i_{kin} = nFAk^\circ C_A^\circ$. Typical plots of i_l^{-1} vs. $\omega^{-1/2}$ at bare electrodes are given in Figures 12a, 13a, and 14a. Diffusion coefficients extracted from the slopes of these lines are given in Table I.

The behavior of polymer-coated RDE's can also be analyzed by plots of i_l^{-1} vs. $\omega^{-1/2}$ [30,32,33] Recently Saveant and co-workers[30] described a model in which several film processes, besides mass transport in solution, could be rate limiting: (1) diffusion of the solution substrate, A [e.g., H_2Q, Fe^{2+}, $Fe(CN)_6^{4-}$] in the film; (2) diffusion-like transfer of charge in the film via the mediator couple, P/Q [i.e., $Ru(bpy)_3^{2+/3+}$]; and (3) the redox reaction between mediator product, Q, and solution species, A. These processes are represented by the characteristic currents:[30b]

$$i_s = FAC_A^\circ\kappa D_s/\phi \quad (6)$$

$$i_E = FAC_p^\circ D_E/\phi \quad (7)$$

$$i_k = FAk_1\Gamma_p^\circ\kappa C_A^\circ \quad (8)$$

(30) The notation used generally follows that in: (a) Andrieux, C. P.; Dumas-Bouchiat, J. M.; Saveant, J. M. *J. Electroanal. Chem.* **1982**, *131*, 1. (b) Andrieux, C. P.; Saveant, J. M. *Ibid.* **1982**, *134*, 163. (c) Andrieux, C. P.; Saveant, J. M. *Ibid.* **1982**, *142*, 1.

(31) (a) Bard, A. J.; Faulkner, L. R. "Electrochemical Methods"; Wiley: New York, 1980. (b) *Ibid.*, Chapter 8.

(32) Anson, F. C.; Saveant, J. M.; Shigehara, K. *J. Am. Chem. Soc.* **1983**, *105*, 1096; *J. Phys. Chem.* **1983**, *87*, 214.

(33) (a) Gough, D. A.; Leypoldt, J. K. *Anal. Chem.* **1979**, *51*, 439. (b) Gough, D. A.; Leypoldt, J. K. *J. Electrochem. Soc.* **1980**, *127*, 1278.

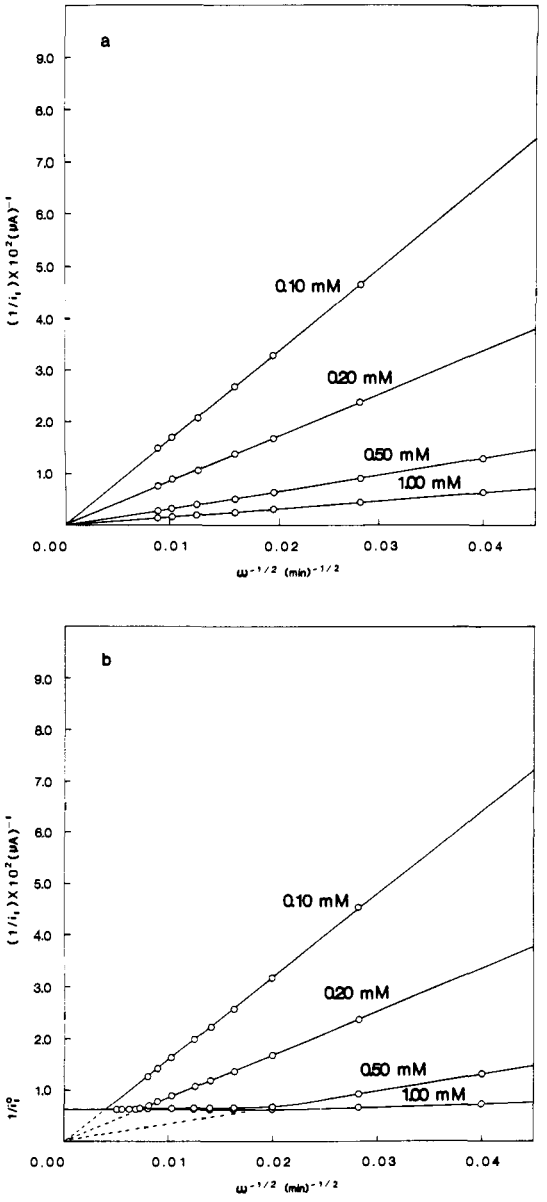

Figure 13. Plots of i_l^{-1} vs. $\omega^{-1/2}$ for the oxidation of hydroquinone in 0.1 M Na_2SO_4: (a) bare GC RDE at $E = +0.7$ V vs. SCE; (b) GC/NAF, $Ru(bpy)_3^{2+}$ ($d = \sim 0.3$ μm) RDE at $E = +1.2$ V vs. SCE.

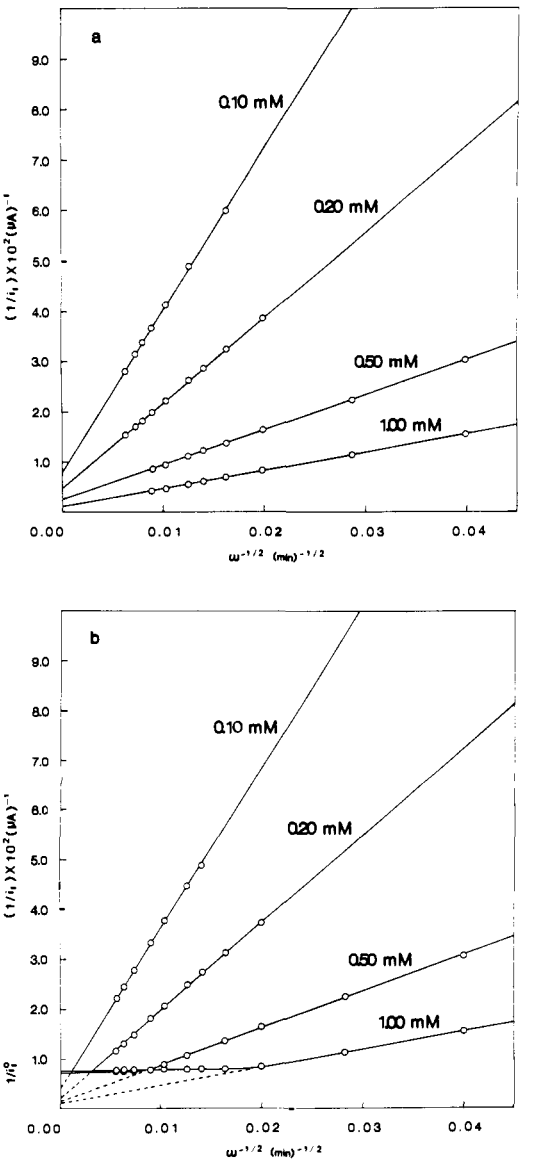

Figure 14. Plots of i_l^{-1} vs. $\omega^{-1/2}$ for the oxidation of $FeSO_4$ in 0.1 M Na_2SO_4 + 0.01 M H_2SO_4: (a) bare GC RDE at $E = +1.05$ V vs. SCE; (b) GC/NAF, $Ru(bpy)_3^{2+}$ ($d = \sim 0.3$ μm), RDE at $E = +1.3$ V vs. SCE.

where D_s and D_E are diffusion coefficients for substrate and electrons in the film, respectively, ϕ is the film thickness, κ is the partition coefficient for substrate between the film and solution, Γ_p° is the surface concentration of mediator (mol cm^{-2}), and k_1 is the rate constant for electron transfer between A and Q. For a substrate that is unable to penetrate the film, clearly $i_s = 0$, and i_k should be expressed as follows:[30a]

$$i_k = FAk_1 \cdot \Gamma_m^\circ \cdot C_A^\circ = FAk_1 \cdot \epsilon \cdot \Gamma_p^\circ / \phi \cdot C_A^\circ = FAk_1' \cdot C_p^\circ \cdot C_A^\circ \qquad (8a)$$

Here Γ_m° is the surface concentration of the mediator in a monolayer adjacent to the film–solution interface, ϵ is the average thickness of the monolayer, and $k_1' = k_1 \cdot \epsilon$ is the second-order reaction rate constant, having the dimension of M^{-1} s^{-1} cm.

The nature of the i_l^{-1} vs. $\omega^{-1/2}$ plots at film-covered electrodes depends upon the relative magnitudes of the characteristic currents.[30b] As shown by the analysis below, the GC/NAF, $Ru(bpy)_3^{2+}$ electrodes with $Fe(CN)_6^{4-}$ in solution follow the case where the substrate does not penetrate the film. For H_2Q and Fe^{2+} in solution, when mediated oxidation occurs, the behavior approximately follows an analogous case. The behavior under these conditions is governed by the equation

$$1/i_l^2 - (1/i_l)[1/i_A + 1/i_E + 1/i_k] + 1/i_A i_E = 0 \qquad (9)$$

This equation can be derived by equating the flux of electrons to the film surface, the rate of reaction between Q and A at the film/solution interface, and the flux of A to this interface. It is the same as that given by Andrieux and Saveant,[30b] but the form of eq 9 is somewhat more convenient for consideration of limiting cases.

For fast electron transfer at the film/solution interface, two limiting cases apply. At slow rotation rates, when the current is mass transfer limited, $i_l = i_A$ (see eq 5) to that the slope of the K–L plot should be the same as at the bare electrode. At high rotation rates, the current becomes limited by charge transport through the film; it is independent of ω and given by $i_l = i_E$ (eq 7). This current is also independent of solution substrate concentration. This same behavior results as the limiting case when the substrate can penetrate the film, the so-called "case E".[30] The other limiting case, when the rate of diffusion of electrons through the film is rapid compared to the interfacial electron transfer, yields the equation:

$$(1/i_l) = (1/i_A) + (i/i_k) \qquad (10)$$

This equation also arises for "case R".[30]

The K–L plots for the $Fe(CN)_6^{4-}$ system given in Figure 12b follow the behavior predicted for this case. At low rotation rates

the slopes in the presence of Nafion are proportional to concentration and yield the same values for the diffusion coefficient in the solution (D_A) as the corresponding plots obtained with a bare electrode (see Table I). At higher rotation rates, $1/i_l$ limits to a value, $1/i_l°$, that is independent of $C_A°$ (it is difficult to attain sufficiently high rotation rates to observe this limiting region at low $C_A°$); this yields $i_E \simeq 135$ μA. Application of eq 7 with appropriate values of ϕ and $C_p°$ [for $Ru(bpy)_3^{2+}$] gives $D \approx 2 \times 10^{-10}$ cm^2 s^{-1}; this is in reasonable agreement with previous estimates based on direct electrochemical measurements of Nafion films containing $Ru(bpy)_3^{2+}$.[25a,b] The observation that the extrapolated lines in the low ω region all show essentially zero intercept, independent of $C_A°$, is consistent with a rapid electron-transfer reaction between $Ru(bpy)_3^{3+}$ and $Fe(CN)_6^{4-}$ at the Nafion/solution interface (see eq 10).

A similar treatment approximately applies for the mediated oxidation of H_2Q at the GC/NAF, $Ru(bpy)_3^{2+}$ electrode (Figure 13b). Although H_2Q can penetrate the film, when the film is loaded with $Ru(bpy)_3^{2+}$ and mediated oxidation occurs (see Figure 9), the total current at this potential essentially represents the mediated oxidation current. Once mediated oxidation starts, the concentration of H_2Q within the film becomes small and the net contribution of penetration of H_2Q to the GC surface becomes small. Thus, cases E or R[30] again apply, and the K–L curves resemble those of the nonpenetrating $Fe(CN)_6^{4-}$ case. Again the slopes of the K–L plots at low ω are proportional to H_2Q concentration and yield D_A values consistent with those at the bare electrode (Table I). Again the intercepts of these plots are essentially zero, indicating fast interfacial charge transfer. The limiting current at high ω is again H_2Q concentration independent and yields $i_E \simeq 1.6 \times 10^2$ μA which is, within uncertainties in ϕ and $C_p°$, essentially the same as that for $Fe(CN)_6^{4-}$. A better approximation for treatment of these data would take into account some penetration of HQ into the film (e.g., the S + E case[30b]); the results obtained in this way are essentially the same as the analysis given above.

The behavior of Fe^{2+} is somewhat different. The K–L plots at a bare electrode with the potential held on the rising portion of the wave produce straight lines with slopes proportional to $C_A°$ (from which D_A values can be obtained) but finite intercepts which reflect the effect of slow heterogeneous electron transfer (Figure 14a). Similar plots taken at more positive potentials yield lines of the same slope but essentially zero intercepts. The presence of a Nafion film appears to facilitate the oxidation of Fe^{2+} (compare curves A and B, Figure 10). This can be attributed to the increased concentration of Fe^{2+} in the Nafion at the GC surface and a change in the nature of the electrode surface; details of this interesting apparent catalytic effect of the thin Nafion film will be discussed elsewhere. The addition of $Ru(bpy)_3^{2+}$ to the film essentially blocks direct penetration of Fe^{2+}, as discussed previously, so that again the model described by eq 9 and its limiting cases applies. Thus, the K–L plots at the GC/NAF, $Ru(bpy)_3^{2+}$ electrode (Figure 14b) again produce lines with slopes proportional to $C_A°$ that yield the same D_A values as the bare electrode (Table I). The limiting current at high ω, $i_E = 137$ μA, is consistent with the values found for $Fe(CN)_6^{4-}$ and H_2Q. Note, however, that for this case, the extrapolated $1/i_l$ vs. $\omega^{-1/2}$ lines at low ω show finite intercepts that are inversely proportional to $C_A°$ (Fe^{2+} concentration in solution). This is consistent with slow interfacial (film/solution) charge transfer as implied by eq 8a and 10. The intercepts yield $i_k/C_A° = 1.7\ (\pm 0.7) \times 10^3$ A mol^{-1} cm^3; this gives, via eq 8a, $k_1' \approx 0.8 \times 10^2$ M^{-1} s^{-1} cm for the interfacial reaction between Fe^{2+} and $Ru(bpy)_3^{3+}$. Note that for zero intercepts of these plots under the conditions of these experiments (i.e., $1/i_k \leq 0.05 \times 10^{-2}$ μA^{-1} at $C_A° = 0.1$ mM), $k_1' \geq 0.8 \times 10^3$ M^{-1} s^{-1} cm.

Luminescence Experiments. The main conclusion from the studies on the electrochemical behavior of polymer bound $Ru(bpy)_3^{2+}$ is that charge transport (diffusion of electrons) through the film becomes limiting as the thickness increases. This accounts for the decrease in photocurrent as the thickness is increased. Luminescence measurements can also provide information about

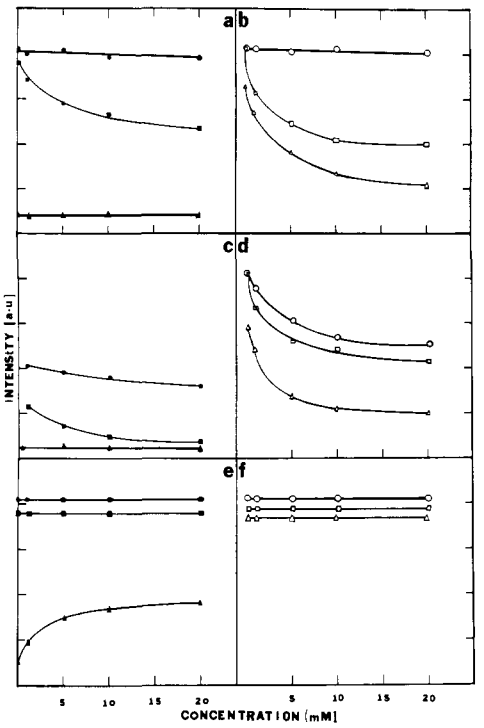

Figure 15. Emission intensity at 600 nm of polymer-bound $Ru(bpy)_3^{2+}$ at various potentials, as a function of supersensitizer concentrations; intensities are normalized to the intensity at +0.2 V in base electrolyte (0.1 M Na_2SO_4) alone. Excitation at 450 nm. Thin films ($d = 0.3$ μm): (a) hydroquinone; (c) $FeSO_4$; (e) $K_4Fe(CN)_6$. Thick films ($d = 3$ μm): (b) hydroquinone; (d) $FeSO_4$; (f) $K_4Fe(CN)_6$. For all cases: (●) +0.2 V vs. SCE, (■) +0.8 V vs. SCE, (▲) +1.4 V vs. SCE.

film processes. Following excitation at the film/solution interface (eq 1), quenching of the excited state by the oxidized or reduced form of the redox couple (eq 11 and 12) is possible; numerous solution- and polymer-phase studies of such processes have been reported.[34,35]

$$Ru(bpy)_3^{2+*} + Red \rightarrow Ru(bpy)_3^{+} + Ox \quad (11)$$

$$Ru(bpy)_3^{2+*} + Ox \rightarrow Ru(bpy)_3^{3+} + Red \quad (12)$$

Moreover, since $Ru(bpy)_3^{3+}$ does not luminesce under these conditions, a measurement of the emission can probe the concentration of the +2 species and the conversion of +3 to +2. We report preliminary studies of the luminescence intensity of film-bound $Ru(bpy)_3^{2+}$ in the presence of different concentrations of the solution redox species, H_2Q, Fe^{2+}, and $Fe(CN)_6^{4-}$ with the electrode held at different potentials (for at least 5 min) before and during the fluorescence measurement. The potentials were chosen so that solution species in the film were either in the oxidized or reduced form so that quenching effects of both forms of the solution species could be studied. Thus, at +0.2 V the system comprises $Ru(bpy)_3^{2+}$ and the reduced form of the solution species, while at +0.8 V the system is $Ru(bpy)_3^{2+}$ and the oxidized form. At +1.4 V both $Ru(bpy)_3^{2+}$ and the solution species are oxidized. The polymer-bound $Ru(bpy)_3^{2+}$ was excited (front side) with 450-nm wavelength light. The emission intensity (front side) at 600 nm was monitored. In Figure 15 the emission intensity as a function of the bulk concentration of the solution species with the electrode at various potentials is shown. The intensities are

(34) (a) Demas, J. N.; Adamson, A. W. *J. Am. Chem. Soc.* **1971**, *93*, 1800. (b) Sabbatini, N.; Balzani, V. *Ibid.* **1972**, *94*, 7587. (c) Boletta, F.; Juris, A.; Maestri, M.; Sandrini, D. *Inorg. Chim. Acta* **1982**, *44*, L175. (d) Bock, C. R.; Meyer, T. J.; Whitten, D. G.; *J. Am. Chem. Soc.* **1974**, *96*, 96. (e) Lin, C. T.; Boltcher, W.; Chou, M.; Creutz, C.; Sutin, N. *J. Am. Chem. Soc.* **1976**, *98*, 6536. (f) Navon, G.; Sutin, N. *Inorg. Chem.* **1974**, *13*, 2159. (g) Sutin, N. *J. Photochem.* **1979**, *10*, 19.

(35) Lee, C. P.; Meisel, D. *J. Am. Chem. Soc.* **1980**, *102*, 5477.

normalized with respect to the intensity at +0.2 V in the absence of any solution species. This quantity was different for thin and thick films and, hence, only the relative magnitudes should be considered. Figure 15a,b are plots of the variation of emission intensity with H_2Q concentration for thin (a) and thick (b) films. At +0.2 V there is very little change in intensity, showing that H_2Q does not quench to any significant extent. At +0.8 V H_2Q is oxidized to benzoquinone and the decreased emission intensity shows that benzoquinone quenches $Ru(bpy)_3^{2+*}$. At +1.4 V, in the case of thin films, most of the $Ru(bpy)_3^{2+}$ is oxidized to the 3+ state as shown by the low intensity in Figure 15a. However, with thicker films a considerable amount of $Ru(bpy)_3^{2+}$ in the film remains in the reduced state, even when the electrode is held at +1.4 V. Quenching still occurs at thick films (Figure 15b) showing that considerable interaction still occurs between the solution- and polymer-bound species at the film/solution interface. Similar results are observed in the case of Fe^{2+}/Fe^{3+}, the only difference being that both Fe^{2+} and Fe^{3+} are capable of quenching $Ru(bpy)_3^{2+*}$ (Figure 15c,d).

$K_4Fe(CN)_6$ exhibits a different behavior. Neither $Fe(CN)_6^{4-}$ nor $Fe(CN)_6^{3-}$ penetrates the Nafion polymer film. However, regeneration of $Ru(bpy)_3^{2+}$ from $Ru(bpy)_3^{3+}$ can occur at the film/solution interface. This happens when the oxidized 3+ species "diffuses" to the film/solution interface, is reduced, and then diffuses back again. (This diffusion occurs by both electron hopping and mass transfer.) Thus, two rate processes can influence the emission intensity. The first one is the diffusion process, which is directly affected by the thickness of the film, and the second is the rate of reconversion at the film/solution interface, which does not directly depend on the thickness. The observed emission intensity will depend on which of the processes dominates under given conditions. The results in Figure 15e suggest that $Fe(CN)_6^{4-}$ is not oxidized at the filmed electrode at +0.8 V, and, hence, no change occurs. At +1.4 V most of the $Ru(bpy)_3^{2+}$ is oxidized to 3+ state at the thin electrode (Figure 15e). However, since electron propagation is faster in thin films, the 3+ ions are reduced back to 2+ at the film/solution interface, thus increasing the emission intensity. At higher concentrations this reconversion becomes more efficient up to 10 mM beyond which electron transport through the film becomes limiting. The situation is very different in the case of thick films (Figure 15f). The oxidation of $Ru(bpy)_3^{2+}$ itself is not very efficient as indicated by the small difference in the luminescent intensity between +0.2 and 1.4 V in the absence of an $K_4Fe(CN)_6$. Secondly, we do not observe any effective reconversion of $Ru(bpy)_3^{3+}$ into the 2+ state. Since the rate of this reaction at the film/solution interface should be independent of film thickness, the absence of effective reconversion supports slow electron propagation in the thick films.

Conclusion

The experimental results obtained in this investigation of the photoelectrochemical properties of Nafion polymer-bound $Ru(bpy)_3^{2+}$ indicate that the decrease in conversion efficiency with increasing film thickness arises mainly from limitations due to charge transport through the film. This transport is associated with a net motion of counterions across the polymer phase to maintain electroneutrality. Albery et al.[26] have shown that for thionine-coated electrodes increasing the anion size decreased the charge-transfer rate through the film. Thus, diffusion of counterions could effectively slow the net propagation of charge. However, previous studies of Nafion films[25c] have shown that the apparent diffusion coefficient for electrons remained the same when the anion size was increased. This result was confirmed for luminescence experiments with electrolytes having bigger anions. Increasing the counterion size did not result in any noticeable decrease in emission intensity for the thin films in the presence of $Fe(CN)_6^{4-}$. If counterion motion was the slow step, increasing the counterion size would hinder electron propagation even in thin films and, thus, the reconversion efficiency.

We have also shown that the efficiency for photosensitization with these polymer electrodes is not improved to any practically important level compared to derivatized electrodes with adsorbed monolayers. Photocurrents are still small ($\sim$nA cm^{-2}). While the efficiency increases slightly with thickness because of improved light absorbance, the increasing film thickness results in increased hindrance of electron flow through the film, which then limits the photocurrent. For Nafion films the optimum thickness appears to be about 0.3 to 0.5 μm.

In many cases the application of polymer electrodes to catalysis appears to be limited by the "film resistance" (i.e., charge propagation through the film). Improvements may be possible in these applications as well as in photosensitization experiments by improving the film conductivity via the incorporation of electronically conductive zones within the film.[25a] Experiments of this type are planned.

Acknowledgment. The authors are grateful to Patrick Leempoel for his help in making luminescence measurements and to Drs. T. Henning, H. White, J. Leddy, D. Ege, J. Saveant, F. Anson, and S. Feldberg for very useful discussions on several aspects of polymer film electrodes. The support of the Robert A. Welch foundation and the National Science Foundation (CHE 8402135) is gratefully acknowledged.

Registry No. SnO_2, 18282-10-5; $Ru(bpy)_3^{2+}$, 15158-62-0; $FeSO_4$, 7720-78-7; $K_4Fe(CN)_6$, 13943-58-3; $Ru(bpy)_3^{3+}$, 18955-01-6; Nafion, 39464-59-0; hydroquinone, 123-31-9; benzoquinone, 106-51-4; carbon, 7440-44-0.

Homonuclear Decoupling in Heteronuclear Chemical Shift Correlation Spectroscopy. 1. Study of Progesterone

Tuck C. Wong* and Venceslav Rutar[†]

Contribution from the Department of Chemistry, University of Missouri, Columbia, Missouri 65211. *Received January 13, 1984*

Abstract: $^1H-^{13}C$ chemical shift correlation spectroscopy was improved by selective reversal of distant protons which eliminates most homonuclear J couplings. The method facilitated easy assignment and separate measurements of ^1H chemical shifts as well as geminal couplings in progesterone. Nonuniform values of one-bond coupling constants $^1J_{CH}$, strong coupling in the proton spin system, and other apparent obstacles against the routine use did not cause serious problems.

Two-dimensional (2D) NMR techniques[1] can provide valuable information about a spin system, but they also require a certain time commitment for data acquisition and processing. Measuring times are especially critical in heteronuclear ($^1H-^{13}C$) versions where signals of low-sensitivity isotopes are detected. Efficiency

[†] On leave of absence from J. Stefan Institute, Ljubljana, Yugoslavia.

(1) Aue, W. P.; Bartholdi, E.; Ernst, R. R. *J. Chem. Phys.* **1976**, *64*, 2229-2246.

0002-7863/84/1506-7380$01.50/0